STUDY OF A LOCAL SURFACE MICRO-DISTURBANCE EFFECTS ON THE SUPERCRITICAL AIRFOIL PERFORMANCE

Wojciech Kania
Aerodynamic Department, Aviation Institute (A.I.)
Al.Krakowska 110/114, 02-258 Warsaw, Poland

Abstract

Deviations from the design conditions of the supercritical airfoil, i.e. higher Mach number or angle of attack, result in the occurrence of shock-wave and corresponding drag rise. Computational and experimental study were undertaken aiming at the extending the limiting boundaries like drag-rise boundary of supercritical airfoil. It was based on a reduction of the shock-wave strength by applying appropriate local disturbance on an airfoil upper surface in form of compression micro-ramp (hump). The 13-percent-thick supercritical airfoil WSA-20 with low moment coefficient, designed at the Aviation Institute, was used as the baseline airfoil. Shape and position of the hump were concluded from the numerical calculations of the transonic flow over the airfoil WSA-20 without and with various humps. The baseline airfoil model and this model with three configurations of the hump were investigated in the A.I. Trisonic Wind Tunnel N-3 at the Mach number range of 0.30-0.86. All airfoil configurations were tested and were compared at approximately the same values of the lift coefficient c_L, what demanded angle of attack adjustment, because the hump changes c_L value at given angle of attack. The reduction of the drag coefficient due to the hump was obtained at the supercritical Mach number, thereby the drag divergence Mach numbers of the tested supercritical airfoil WSA-20 with hump were increased. It was found that the tested compression micro-ramps have only little effects on the low-speed aerodynamic characteristics of the supercritical airfoil WSA-20.

Nomenclature

- c - airfoil chord length
- c_L - lift coefficient
- c_D - drag coefficient from wake measurement
- c_M - pitching moment coefficient about quarter of chord
- c_P - pressure coefficient
- c_{Pte} - trailing edge pressure coefficient (measured at point of 0.98 chord length from leading edge)
- M - Mach number
- M_l - local Mach number on airfoil surface
- M_{DD} - drag divergence Mach number (based on drag coefficient rise of 0.002 above subcritical value)
- M_{BO} - onset of shock -induced separation Mach number (based on $c_{Pte} = 0.1$)
- Re - Reynolds number (based on airfoil chord)
- x - chordwise distance from leading edge
- α - angle of attack

Subscript

- ∞ - freestream condition

Introduction

In performing manoeuvres subsonic combat aircraft often flies in the transonic regime for a significant amount of time. In transonic flow the interaction between shock-wave terminated supersonic region and boundary layer causes drag rise and with increasing Mach number or angle of attack leads to boundary layer separation, which constitutes additional drag rise. The unsteady pressure excitations associated with flow separation due to shock wave can also induce high levels of buffeting. The buffet loads due to flow separation on the wing may cause serious fatigue problems of an aircraft. Additionally, manoeuvrability, performance and handling qualities are very often degraded. For a transport aircraft the drag divergence and buffet onset boundaries are also important characteristics, because they allow aircraft designer to specify the cruise conditions.

A postponement of the flow conditions (Mach number or lift coefficient) on a wing or an airfoil at which significant increase in drag and buffet onset occur is highly desirable. The achievement of this postponement would require the control of either the shock strength or the boundary layer, because control of one leads to an overall change in the interaction due to the interactive nature of the both. The boundary layer can be controlled by a mass transfer in the interaction region. It can be accomplished by active means, as blowing or boundary layer suction. Either blowing or suction requires power, thus active control is limited by the fact that an extra pump drag should be added to the total drag of the airfoil. The other control technique is the passive control of shock-boundary layer interaction (PCSB)[1]. This technique consists of placing in the shock region a porous plate with a vent chamber installed beneath it. The large pressure difference over the

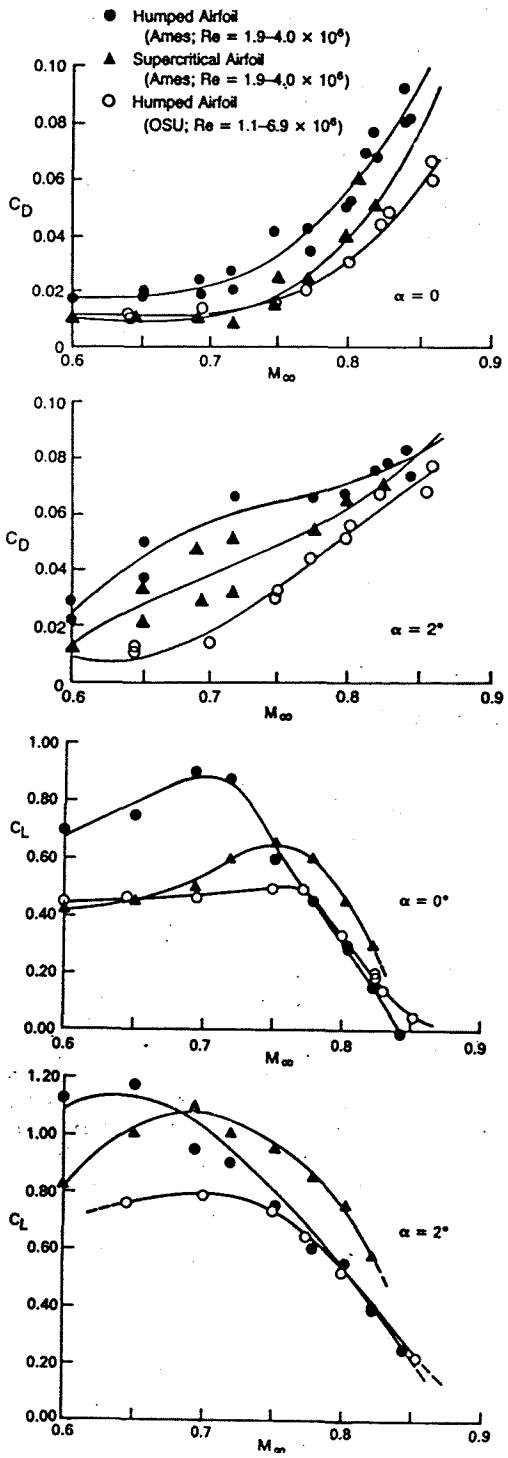

Fig. 1 Drag and lift characteristics of Korn-Garabedian supercritical airfoil without and with hump investigated at the NASA Ames and OSU from Ref.7

shock-wave will result in a natural flow circulation through the cavity from downstream to upstream of the shock-wave. The air blowing process produces a rapid thickening of the boundary layer approaching the shock, which in turn generates a system of weaker shocks. This leads to reduction of the airfoil wave drag, and the drag rise Mach number is increased. Many experimental tests[2-6] demonstrated that PCSB technique can be effective in improving the transonic airfoil performance.

A very simple concept to improve the transonic performance of supercritical airfoil at off-design conditions was introduced by Tai T.T. et. all.[7]. This concept consists of placing a small compression ramp, named hump, with sharp corner on the rear upper surface at the shock location of the supercritical airfoil. A 16-percent-thick Korn-Garabedian supercritical airfoil was used as the baseline airfoil. The experimental investigation has been conducted in the transonic wind tunnels at NASA Ames Research Centre and Ohio State University. The experimental results , which are shown in fig. 1, did not allow to make reliable conclusion concerning the effects of the hump on the drag coefficients and drag divergence boundary of tested supercritical airfoil. It may be explained by a fact that all compared airfoils were tested at the same angle of attack but at different values of lift coefficient, (as it is shown in fig. 1), whereas the hump causes a significant change of the tested supercritical airfoil lift coefficient. It was concluded, only, that the level of drag divergence was more moderate in the case of the humped airfoil than of the baseline supercritical airfoils.

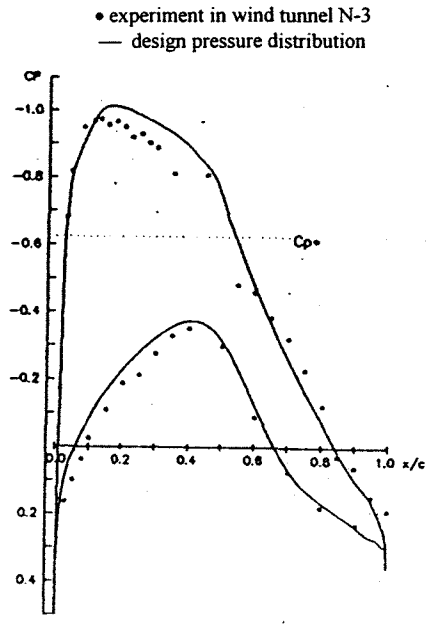

Fig. 2 Design pressure distribution of superctritical airfoil WSA-20 at M=0.74 and c_L=0.46 tested in the A.I. Trisonic Wind Tunnel N-3.

This paper describes computational and experimental study, which was undertaken at the A.I.[8], to verify concept of extending the limiting boundaries i.e. drag divergence and buffet onset boundaries of a supercritical airfoil by applying appropriate local disturbance of airfoil upper surface in form of compression micro-ramp (hump). The 13-percent- thick supercritical airfoil WSA-20, designed and tested in the wind tunnel at A.I.[9-11], was used as the baseline airfoil. The design pressure distribution of this airfoil at Mach number of 0.74 and lift coefficient of 0.46 is shown in fig. 2. The noteworthy aerodynamic feature of the WSA-20 airfoil is low value of the moment coefficient partly due to reduction of the airfoil rear loading. The shape and position of the hump was determined from the numerical computation of the viscous transonic flow over the airfoil WSA-20 without and with various configurations of the hump. It is very important to note that all airfoil configurations were tested and were compared in transonic regime at approximately the same value of the lift coefficient, what demanded angle of attack adjustment.

Experimental Investigation

Test Facility

The experimental results presented in this paper were obtained from tests performed in the A.I. Trisonic Wind Tunnel N-3. The N-3 is a intermittent blowdown wind tunnel with partial recirculation of the air and Mach number range of 0.2÷2.3. At subsonic and transonic speeds, Mach number can be varied continuously from 0.2 to 1.15 with independent control of Mach and Reynolds numbers by means of the stagnation pressure variation. Reynolds number can be varied from $16 \cdot 10^6$ to $32 \cdot 10^6$ [1/m] at Mach number of 1.0. The test section has a 0.6x0.6 metre square cross section, 2 metre in length. The bottom and top walls are perforated, and the side walls are solid. For airfoils test the N-3 wind tunnel is equipped with the pressure scanning system (SCANIVALVE SGM-48 for 192 pressure points), a wake multipoint pressure rake, a b/w or coloured Schlieren flow visualisation system. The control of the flow, measurements and data acquisition/processing are carried out by SPITA N-3 system based on two PC486 processors.

Model and Measurements

The investigated models were the advanced supercritical airfoil WSA-20 without and with three configurations of the hump. The humps peak were located at range of x/c position 57% - 60% measured from the airfoil leading edge. A choice of the hump positions was based mainly on the experimentally obtained flowfield over the baseline airfoil at the range of angles of attack from 1° to 3°. The heights of the humps were ranged from 0.06% to 0.15% (0.1 mm÷0.25 mm) of the airfoil chord length. It was deduced from above mentioned transonic flow calculations over the supercritical airfoil WSA-20 with many configurations of the hump. The front part of the hump was shaped as a compression ramp with length of approximately 6% - 9% of the chord length, depending on the hump configuration. The tested hump configuration were designated :

$$h/x_h ,$$

were : h - height of the hump peak in percent of the chord length,

x_h - position of the hump peak from leading edge in percent of the chord length.

The 13-percent-thick model spanned the entire test section width of 0.6 m was installed between the optical windows embedded in the test section walls and was fixed in a mechanism of an angle of attack change. The model had a airfoil chord of 170 mm resulting in span/chord and tunnel height/chord ratios of 3.5. Forty-four pressure taps (28 on upper and 16 on lower surfaces), each having a 0.4 mm diameter, are located along the midspan. The lift and moment were obtained by integrating the pressure distribution on the airfoil surface. The drag data were computed by integration of total and static pressures obtained from the 120 points wake pressure rake located one chord length downstream of the airfoil trailing edge. The pressure on the airfoil surface and in the wake for each position of the scanivalve were measured simultaneously with freestream parameters. All presented data were corrected for the effects of the blockage and the lift interference. The correctness of applied testing technique and procedure was confirmed by calibration test of the NACA 0012 airfoil[12], which results are in a good agreement with data presented by McCrosky[13]. The onset of shock-induced separation was determined from the variation of the pressure coefficient at the tap on the airfoil upper surface closest to trailing edge (0.98·c) versus Mach number for the constant angle of attack. The experimental investigation, besides surface and wake pressure distributions, was included coloured Schlieren photographs of flow visualisation, as well.

Test range and conditions

The presented tests covered a Mach number range from 0.3 to 0.84 with corresponding Reynolds number, based on chord length, from $1.2 \cdot 10^6$ to $3.0 \cdot 10^6$. At subsonic Mach number up to 0.6 the tests were conducted at constant Mach number for angle of attack range from -4° to 11÷14.5° depending on Mach number. At transonic regime the Mach number was varied at several constant angle of attack in range from -2° to 5°. All airfoil configurations without and with humps at transonic speeds were tested and results were compared at approximately the same values of lift coefficient. This approach was applied due to the fact that the lift coefficient is depended on the hump and its geometry. The tests were conducted with free transition of the boundary layer, but it was

checked that at all tested cases the boundary layer was turbulent at region of interaction with shock-wave.

Results and Discussion

Comparison of the supercritical airfoil WSA-20 drag coefficient without and with hump of 0.06% chord height in the Mach number range of 0.7 to 0.82, shown in Fig. 3, indicates that the smallest hump is ineffective in a change of the drag characteristic.

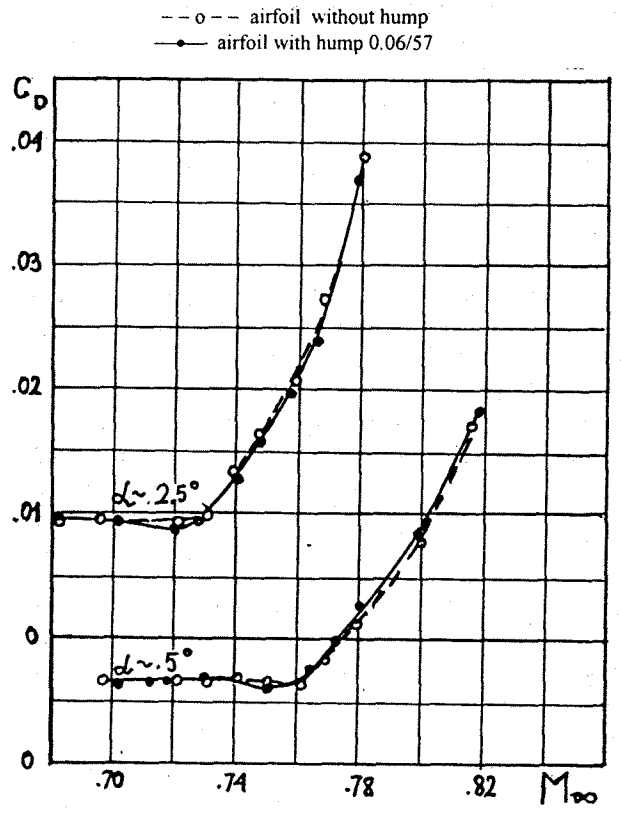

Fig. 3 Effect of hump 0.06/57 (heihgt of 0.065 chord /positon of chord) on drag coefficient of supercritical airfoil WSA-20 - test in wind tunnel N-3 at Re=2.7·10^6.

In Fig. 4 the drag coefficient of the airfoil with greater humps (heights of 0.1% and 0.15% chord length) in the Mach number range of 0.7 to 0.84 are compared with the baseline airfoil results at a lift coefficient of 0.3 to 0.7. The compared results were obtained at approximately the same values of the lift coefficient, as is shown in Fig. 5. For both above mentioned humps a favourable effect on the drag coefficient was obtained. Fig. 4 demonstrates, that the humped airfoil drag coefficients are decreased in comparison with the baseline airfoil at Mach numbers greater than the baseline airfoil drag divergence boundary. The drag divergence Mach numbers of the humped airfoils are greater than the baseline airfoil. It leads to an extension of the drag divergence boundary $c_L(M_{DD})$ of the humped supercritical airfoil WSA-20 in lift coefficient range 0.10 to 0.65, as is shown in Fig.7.

The influence of the humps on the supercritical airfoil trailing-edge pressure coefficient (measured at point 0.98 x/c) as a function of freestream Mach number is shown in Fig. 6 at several angles of attack giving approximately equal lift coefficient values of tested airfoil model without and with the humps (see Fig. 5) . The divergence of the trailing-edge pressure coefficient, which may be regard as a indication of a shock-induced separation, is shifted due to the hump toward higher Mach numbers. It is favourable effect of the investigated humps on shock/boundary-layer interaction. At Mach numbers lower than the trailing edge pressure divergence Mach number the hump exhibits no effect on the trailing-edge pressure coefficient. The onset of shock-induced separation boundary was determined based on the trailing-edge pressure coefficient c_{Pte} and lift coefficient data presented in Fig. 6 and 5, and on the criterion $c_{Pte} = 0.1$. Fig. 7 shows the shock-induced separation onset boundaries for the baseline airfoil and two humps configurations of 0.1% and 0.15% c heights. It is seen that the tested supercritical airfoil shock-induced separation boundary is extended due to the hump at the lift coefficients lower then 0.6. At given Mach number the hump causes the shock-induced separation lift coefficient increase of about 0.1 in the lift coefficient range up to 0.4.

In Fig. 8 the humped airfoil moment coefficients as a function of Mach number are compared with the baseline airfoil results. It is seen no effect of the hump on moment coefficient throughout the tested range of Mach numbers and angles of attack.

Comparisons of a typical Mach number M_l distribution on the surface of the airfoil without and with the hump are shown in Fig. 9. It can be stated that the noticeable effect of the hump on the Mach number distribution has a local character only. The measured Mach number M_l distributions differ only in the shock region, where the Mach number distribution is distinctly flattened due to the hump or even small compression occurs. The hump reduces a shock Mach number, what means a reduction of shock-wave strength. Schliren photographs show that the hump causes spliting a single shock wave into system of weaker shocks. It allows to draw a conclusion that the supercritical airfoil drag reduction is mainly due to the softening of the shock-wave caused by the hump. It should be noticed that this drag reduction occurs even at values of shock Mach number lower then 1.3, whereas to obtain a net reduction in drag by PCSB shock Mach number should be equal or greater than 1.3, as it is stated by Raghunathan[1]. At shock Mach number greater than 1.3, the hump causes also other changes in the Mach

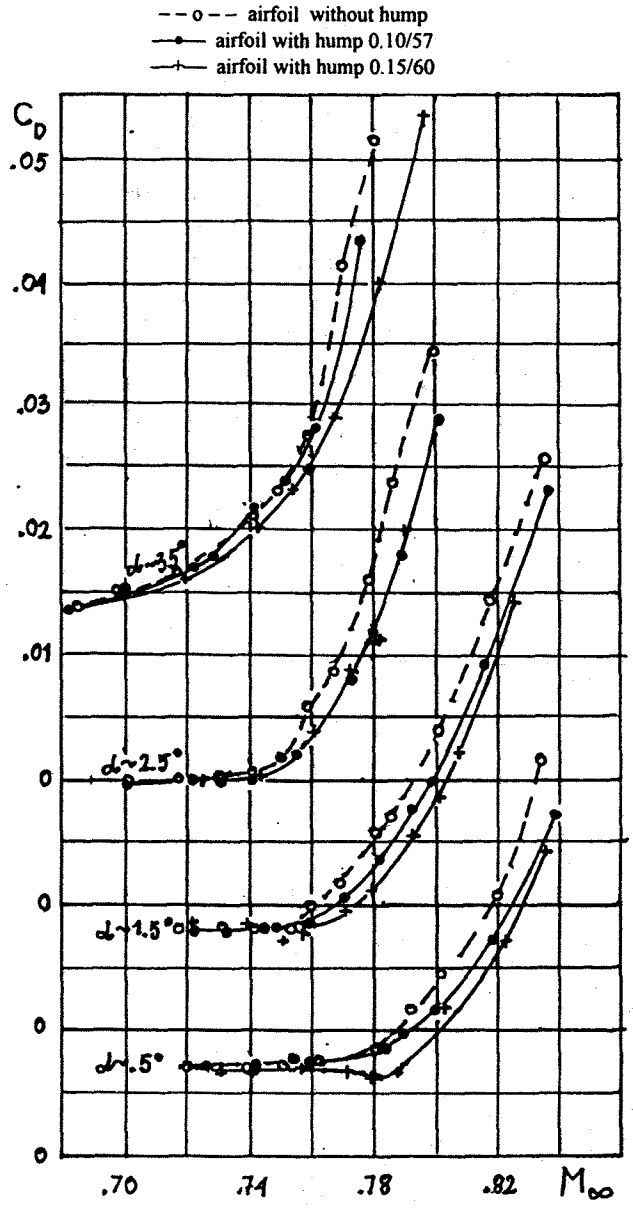

Fig. 4 Effect of humps 0.10/57 and 0.15/60 on drag coefficient of supercritical airfoil WSA-20 - test in wind tunnel N-3 at $Re=2.7\cdot10^6$ and lift coefficient presented in Fig. 5.

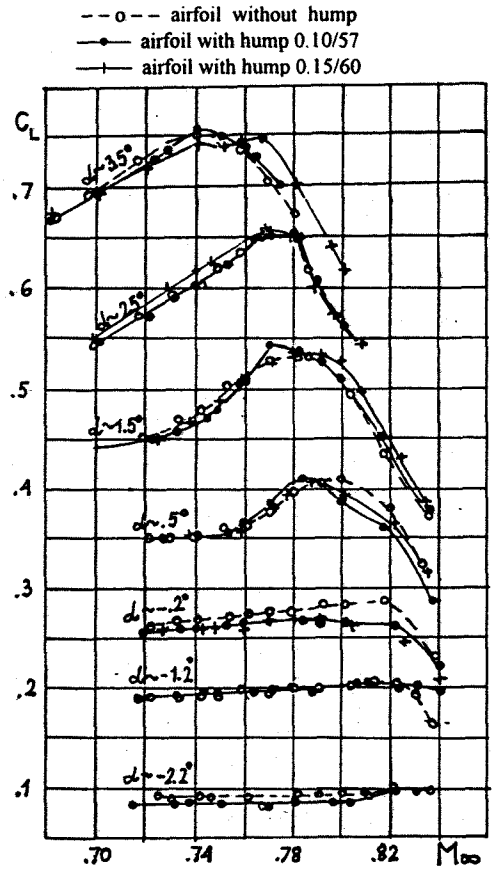

Fig. 5 Lift coefficients at which supercritical airfoil WSA-20 without and with of humps 0.10/57 and 0.15/60 were tested in wind tunnel N-3 at $Re=2.7\cdot10^6$.

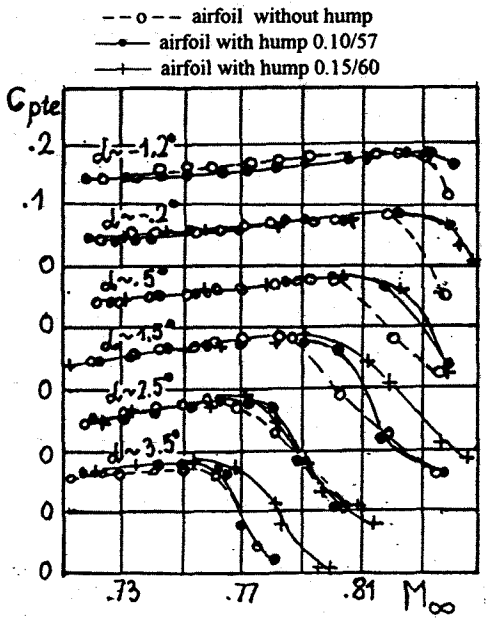

Fig. 6 Effect of humps 0.10/57 and 0.15/60 on trailing edge pressure coefficient of supercritical airfoil WSA-20 test in wind tunnel N-3 at $Re=2.7\cdot10^6$ and lift coefficient presented in Fig. 5.

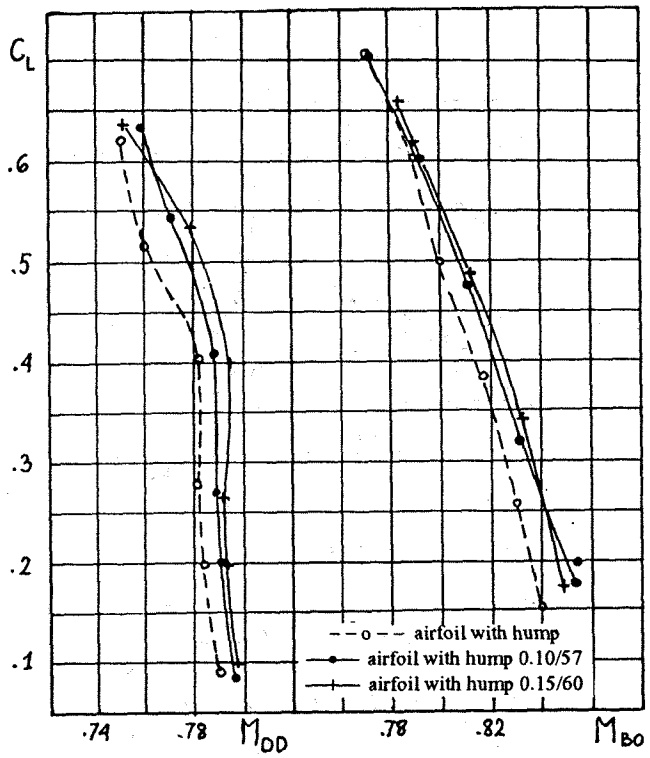

Fig. 7 Extension of drag divergence and shock-induced separation onset boundaries of supercritical airfoil WSA-20 due to the humps 0.10/57 and 0.15/60.

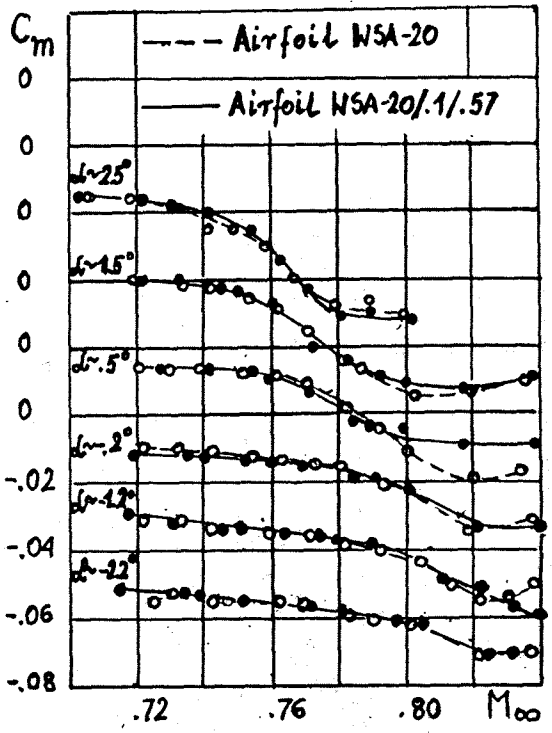

Fig. 8 Effect of humps 0.10/57 and 0.15/60 on pitching moment coefficient of supercritical airfoil WSA-20 - test in wind tunnel N-3 at $Re=2.7 \cdot 10^6$ and lift coefficient presented in Fig. 5.

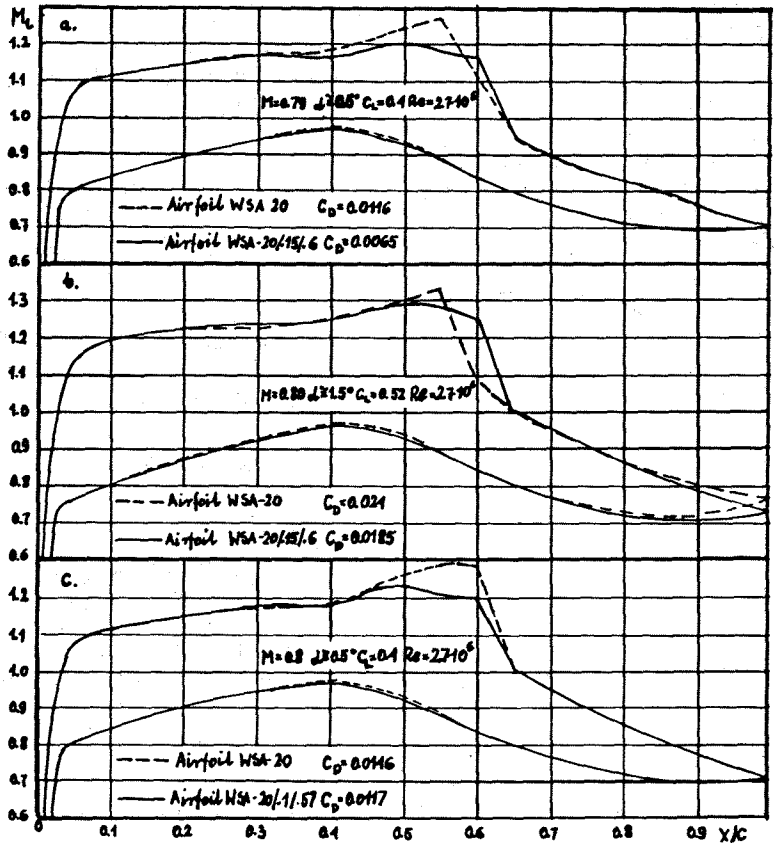

Fig. 9 Effect of humps 0.10/57 and 0.15/60 on Mach number distribution on supercritical airfoil WSA-20 surface - test in wind tunnel N-3.

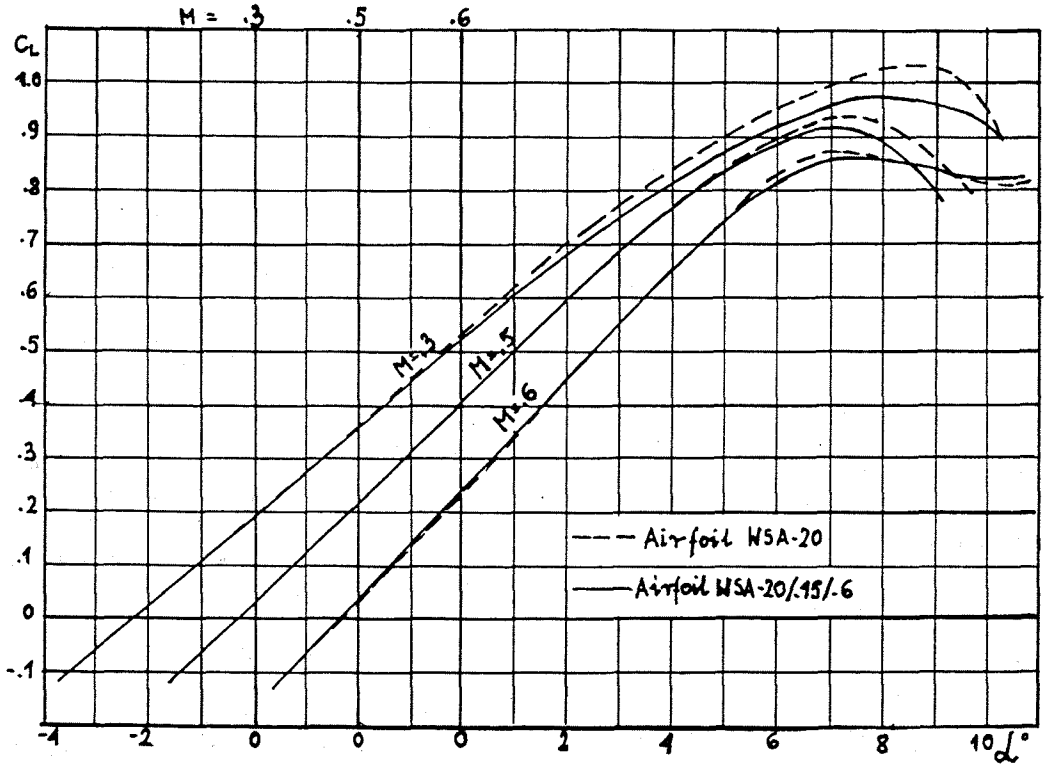

Fig.10 Effect of hump 0.10/57 and 0.15/60 on lift coefficient of supercritical airfoil WSA-20 at low Mach number - test in wind tunnel N-3 t M = 0.3, 0.5, 0.6 anr Re = 4·M·10^6.

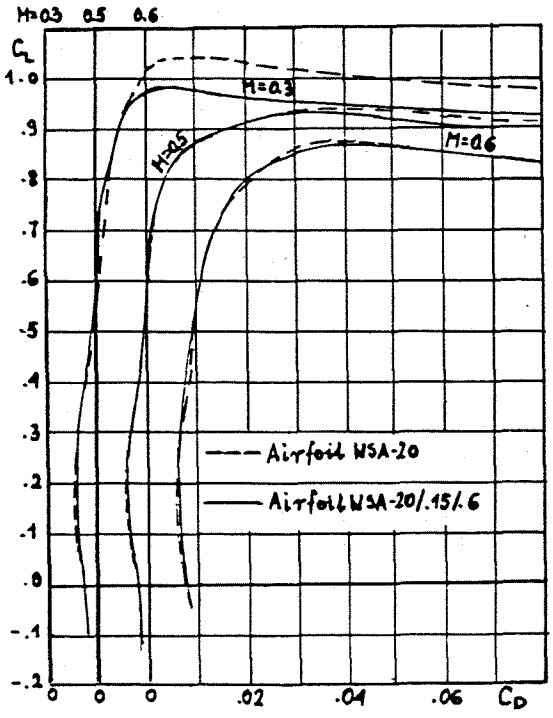

Fig.11 Effect of hump 0.10/57 and 0.15/60 on Mach number distribution on supercritical airfoil WSA-20 surface - test in wind tunnel N-3 at M = 0.3, 0.5, 0.6 anr Re = 4·M·10^6.

number distribution, as it is shown in Fig. 9b. The first change concerns to values of the Mach number immediately behind the shock-wave, which on the baseline airfoil becomes greater then 1.0. According to Stanewsky[14] it indicates the occurrence of the rapid extension of a shock-induced separation bubble. The occurrence of shock-induced separation extended to the trailing edge on the baseline airfoil at considered conditions (M_∞=0.80 and c_L=0.52) - see Fig. 9b - can be confirmed by a upstream shock-wave movement and a divergence of trailing edge Mach number. Due to the effect of the hump on shock-boundary layer interaction mentioned above parameters undergo changes: Mach number immediately behind the shock is lower than 1.0, the shock does not move upstream and trailing edge Mach number of the supercritical airfoil with the hump is lower than of the baseline airfoil. These confirme that the shock-induced separation on the supercritical airfoil is delayed due to the hump.

Beside test at transonic range, the supercritical airfoil WSA-20 without and with three configurations of the hump were investigated at low Mach number range of 0.3-0.6 aiming at determination of possible unfavourable hump effects. Fig. 10 and 11 summarise the effects of the biggest hump 0.15/60 on a aerodynamic characteristics of the supercritical airfoil WSA-20. Fig. 10 demonstrates that the hump causes a little reduction of a maximum lift coefficient. This reduction is diminished with increase of

Mach number and with decrease of the hump height. A drag polars of baseline airfoil and airfoil with hump 0.15/60 are compared in Fig. 11 at Mach numbers of 0.3 to 0.6. It may be concluded that the effect of the hump on the drag coefficient is negligible at Mach number lower than 0.6.

Conclusions

The present study was aiming at possible improvement of a supercritical airfoil transonic performance by applying appropriate local micro-disturbance on airfoil upper surface in form of a compresion ramp (hump). The experimentally tested humps geometry and position were determined based on numerical results of the hump effect on transonic performance of baseline supercritical airfoil and experimental flowfield over this airfoil. The results of the conducted experimental wind tunnel test allow to make some general conclusions:

1. The hump of 0.06% chord height exhibits no effect on transonic performance of the supercritical airfoil.
2. The aerodynamic performance of supercritical airfoil can be improved by the hump of appropriate geometry parameters, i.e. height at least of 0.10% chord and compresion ramp length of 8% to 9% chord.
3. The hump reduces the drag coefficient of the supercritical airfoil, leading to an extension of the drag divergence boundary. These favourable effects are mainly due to a reduction of shock-wave strength caused by the hump.
4. The supercritical airoil drag reduction occurs even at shock Mach number lower then 1.3, whereas a drag reduction by PCSP can be obtained at Mach number equal or greater than 1.3.
5. The supercritical airfoil shock-induced separation onset is delayed due to the hump at the lift coefficient lower than 0.6.
6. The tested hump does not effect on the supercritical airfoil moment coefficient.
7. At low Mach number range $M \leq 0.6$ the tested hump has only little effects on the supercritical airfoil aerodynamic characteristic.

Acknowledgements

The work reported in this paper was carried out with a support of the State Committedd for Scientific Resaerch (KBN), which the author is grateful to acknowledge. The author woud like to thank Mrs B. Zwierchanowska, Mr J.Żółtak and Mr A. Laskowski for their help in the preparation of this paper.

References

1. Raghunathan S., "Passive control of shock-boundary layer interaction", Prog.Aerosp.Sci., Vol. 25, No 3, 1988, p.271-296.
2. Krogmann P., Stanewsky E., Thied P., " Effects of suction on shock-boundary layer interaction and shock-included separation", J.Aircraft, No 1, 1985, p.37-42.
3. Chokani N., Squire L.C., "Passive control of shock/boundary layer interactions: numerical and experimental studies", IUTAM Symposium Transonicum III, Springer Verlag, 1989, p.399-406.
4. Thiede P., Krogmann P., „Passive control of transonic shock/boundary layer interaction", ibid, p.379-388.
5. Raghunathan S., Mc Ilwain S.T., "Further investigation of transonic shock-wave/boundary-layer interaction with passive control", J.Aircraft, No 1, 1990, p.60-65.
6. Bur R., "Passive control of a shock-wave/turbulent boundary layer interaction in a transonic flow", Rech.Aerosp., No 1992-6, 1992, p.11-30.
7. Tai T.C., Huson G.G., Hicks R.M., Gregorek G.M., "Transonic characteristic of a humped airfoil", J.Aircraft, No 8, 1988, p.673-674.
8. Kania W., „Study of modified concept of supercritical airfoil", Internal Report of the A.I., No 1/BA/93/P, 1993, (in Polish).
9. Kania W., Stalewski W., "Numerical design of the supercritical airfoils of the I-22M aircraft", Internal Report of the A.I., No 25/BA/90/H, 1990, (in Polish).
10. Skowroński J., "Wind tunnel test on the supercritical airfoils of the I-22M aircraft", Internal Report of the A.I., No 32/BA/90/H, 1990, (in Polish).
11. Kania W., "Development of supercritical wing trainer/combat jet aircraft", Proceeding of XI Conference on Fluid Mechanics, Warsaw, 1994, p 267-275 (in Polish)
12. Krzysiak A., Zwierchanowska B., "Results of the tests on NACA 0012 airfoil, ONERA M2 and CAGI calibration models in the A.I. Trisonic Tunnel N-3, Internal Report of the A.I., No 88/BA/94/D, 1994, (in Polish).
13. McCroskey W.J., "A critical assessment of wind tunnel results for the NACA 0012", Paper 1, AGARD CP No. 429,1987
14. Stanewsky E., "Interaction between the outer invicid flow and the boundary layer on transonic airfoils", Zeitschrift Flugwiss. Weltraumforsch., Vol. 7, No. 4, 1983, pp.242-252